4. ANKARA INTERNATIONAL AEROSPACE CONFERENCE AIAC-2007-051
10-12 September, 2007 - METU, Ankara

EVALUATION OF CLOSURE HYPOTHESES USING RECENT EXPERIMENTAL DATA ON THE SIMILARITY REGION OF SWIRLING JET FLOWS

Abolfazl F. Shiri* and William K. George†
Chalmers University of Technology
Gothenburg, Sweden

Sara Toutiaei‡
University of Wyoming
Laramie, WY, USA

ABSTRACT

An experimental recent study by Shiri et al.[2] using laser Doppler anemometry showed that the growth rate enhancement due to swirl (c.f. Gilchrist, Naughton [3]) does not persist in the far-field of a swirling jet flow with moderate swirl numbers (0.15 and 0.25). The results were consistent with the equilibrium similarity theory of Ewing [4] in which the mean swirl velocity was argued to decrease downstream as $1/(x-x_o)^2$, while the mean stream-wise velocity decreased as $1/(x-x_o)$. The investigation included all three velocity components of the turbulence quantities at a swirl number of $S=0.25$, and all moments to third order were obtained (except those involving both the azimuthal and radial components simultaneously). As noted by George [8], if there were an effect of the source conditions on the similarity profiles, it is in the second and higher moment profiles where it would be expected to appear. The second and third-order moments are quite close to the earlier non-swirling results; some are collapsing perfectly, others have a slight difference. Regardless, the results are of considerable interest, since many of the quantities measured are those which must be modeled in all second-order closure models. This evaluation is of particular interest since both the mean azimuthal and mean radial velocities were obtained directly, meaning that both continuity and momentum balances were possible. The primary goal of this paper was originally to carry out such evaluations, but that work is still in progress. Here the swirl is shown to have a negligible effect on the overall Reynolds normal and shear stress balances.

INTRODUCTION

For many years researchers have been interested in turbulent jets, both because of their numerous applications as well as their importance to our fundamental understanding of turbulence. Swirling jets add to the interest of this class of flows because swirl can be considered as a significant change in the jet flow's initial conditions and many experimental and theoretical studies have tried to address the questions of the stability and dependency on initial condition of jet flow. Farokhi et al. [7] and Gilchrist and Naughton [3] investigated the effect of swirl on the near-field flow of an axisymmetric jet and showed that moderate swirl (below vortex breakdown) enhances the growth rate and mixing compared to those of a non-swirling jet.

By contrast, our own earlier results (Shiri et al. [2]), were shown to be consistent with the equilibrium similarity theory of Ewing [4] in which the mean swirl velocity was argued to decrease downstream as $1/(x-x_o)^2$, while the mean stream-wise velocity decreased as $1/(x-x_o)$. In fact the only statistically significant effect of the swirl on the mean velocity for even the highest swirl number was a shift in the virtual origin (to $x/D_*=0.75$ from -2.9) as shown in Figure 1.

*Ph.D. Student in Applied Mechanics Department, Email: abolfazl@chalmers.se
†Prof. in Applied Mechanics Department, Email: wkgeorge@chalmers.se
‡Ph.D. Student in Applied Mechanics Department, Email: toutiaei@uwyo.edu

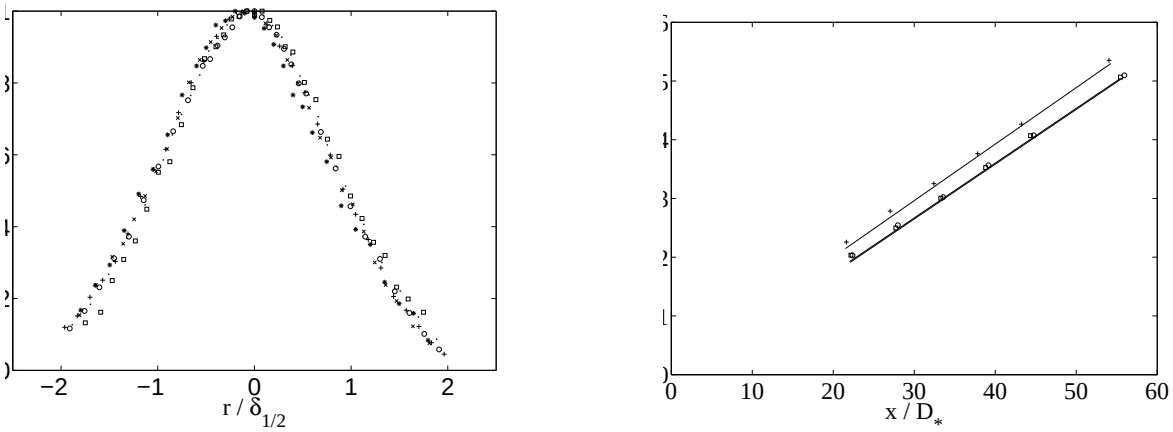

(a) Normalized mean stream-wise velocity profiles at $x/D = 20, 25, 30, 35, 40, 50$.

(b) Stream-wise variation of the velocity profiles half-width. S: 0, 0.15, 0.25; Slopes: 6.87, 6.86, 6.81; Virtual origins: 0.755, 0.754, -2.859

Figure 1: Mean axial velocity

Momentum Equations

The Navier-stokes equations in cylindrical coordinate, ignoring the viscous terms, are given by:

$$U\frac{\partial U}{\partial x} + V\frac{\partial U}{\partial r} = -\frac{1}{\rho}\frac{\partial P}{\partial x} - \frac{\partial \overline{u^2}}{\partial x} - \frac{\partial \overline{uv}}{\partial r} - \frac{\overline{uv}}{r} \tag{1}$$

$$-\frac{W^2}{r} = -\frac{1}{\rho}\frac{\partial P}{\partial r} - \frac{\partial \overline{uv}}{\partial x} - \frac{\partial \overline{v^2}}{\partial r} + \frac{\overline{w^2} - \overline{v^2}}{r} \tag{2}$$

$$U\frac{\partial W}{\partial x} + V\frac{\partial W}{\partial r} + \frac{VW}{r} = -\frac{\partial \overline{uw}}{\partial x} - \frac{\partial \overline{vw}}{\partial r} - 2\frac{\overline{vw}}{r} \tag{3}$$

These equations can be integrated over a plane downstream of the jet to derive axial and angular integral momentum equations given below:

Conservation of axial momentum in axial direction:

$$M_0 = 2\pi \int_0^\infty \left[U^2 - \frac{W^2}{2} + \overline{u^2} - \left(\frac{\overline{w^2} + \overline{v^2}}{2} \right) \right] r dr \tag{4}$$

Conservation of angular momentum in axial direction:

$$G_\theta = 2\pi \int_0^\infty [UW + \overline{uw}] r^2 dr \tag{5}$$

These show expressing that the integrated axial and angular momentum fluxes are conserved as the jet evolves downstream. We can define the ***swirl number*** as a characteristic of the strength of the swirling jet:

$$S = \frac{G_\theta}{M_0 R} \tag{6}$$

Clearly it can be interpreted as a ratio of the length scale, G_θ/M_0, to the jet radius, R.

EXPERIMENTAL SETUP

The existing facility used by Hussein et al.[5] was modified to produce both axial and tangential velocity at the exit. The jet exit profile was nearly a top-hat [2] . Two ***fifth-order polynomial*** contraction was used, as it is shown in Figure 2, to convert the tunnel diameter into the jet exit diameter $D = 25.4mm$ (one inch). One main blower was used to supply axial flow, and six 15 mm injectors connected to a second blower added the swirling component independently. The facility was confined in a tent of size of $10m \times 3.5m \times 3.5m$. A two-component Laser Doppler Anemometry method was used to measure instantaneous velocity field. Measurement was carried out in different cross-sections of the jet, but the data presented here were taken in the far-field of the jet $(30D)$ where the jet has

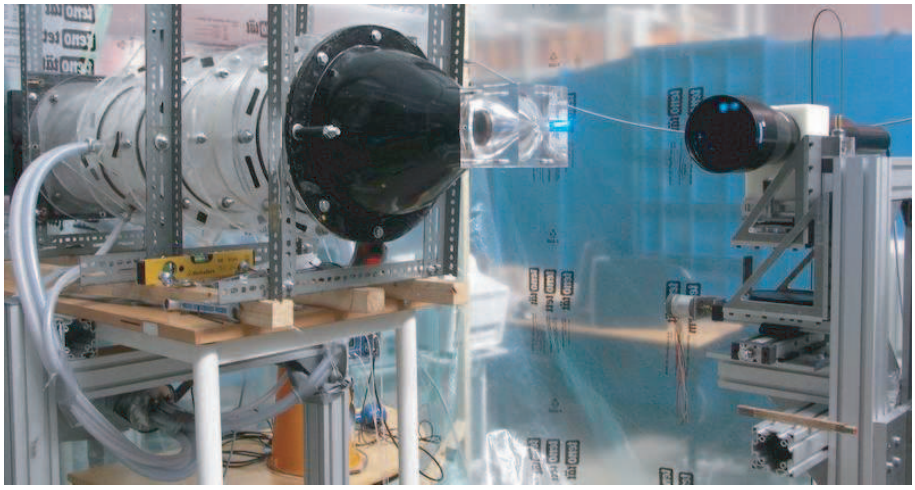

Figure 2: Swirling Jet Facility Setup.

a self-preserving behavior for a swirling jet with swirl number $S = 0.25$. More detail about the experiment can be found in Shiri et al. [2].

RESULTS

The Reynolds stresses $\overline{u^2}, \overline{v^2}, \overline{w^2}$ and $\overline{uv}$ are plotted in figure 3. The values are normalized by the square of the centreline velocity at the cross-section and compared with the results from non-swirling jet produced by the same facility with Hussein et al. [5]. Third-order moments are also plotted in figure 4 and compared with the non-swirling data. Curve fits to these data are provided in tables 1 and 2. With a single exception, $\overline{uw^2}$, the profiles of all moments are in excellent agreement with the earlier results, except for a slight decrease in those involving the u-component which are slight lower [1]. The reason for this is not know at this point.

Table 1: Curve fits for even functions, $f(\eta) = [C_0 + C_2\eta^2 + ...]e^{A\eta^2}; (\eta = r/(x - x_0))$.

-	C_0	C_2	C_4	C_6	A
$\overline{u^2}$	1.587	330.284	−1922.685	878055.498	156.166
$\overline{v^2}$	1.048	53.648	0.066	–	86.364
$\overline{w^2}$	1.032	129.134	−2159.596	52742.686	104.112
$\overline{u^3}$	0.2	146.908	9861.882	−2.579	135.747
$\overline{uv^2}$	−0.172	106.123	−756.518	449688.093	172.189
$\overline{uw^2}$	−0.177	33.640	3474.348	1.342	142.374

Table 2: Curve fits for odd functions, $f(\eta) = [C_1 + C_3\eta^3 + ...]e^{A\eta^2}; (\eta = r/(x - x_0))$.

-	C_1	C_3	C_5	C_7	A
$\overline{uv}$	−11.946	−424.067	−34742.577	−1390539.741	173.261
$\overline{u^2v}$	3.418	−2275.911	99175.818	−8126140.636	197.919
$\overline{v^3}$	−3.9411	−488.044	−2.967	–	111.377

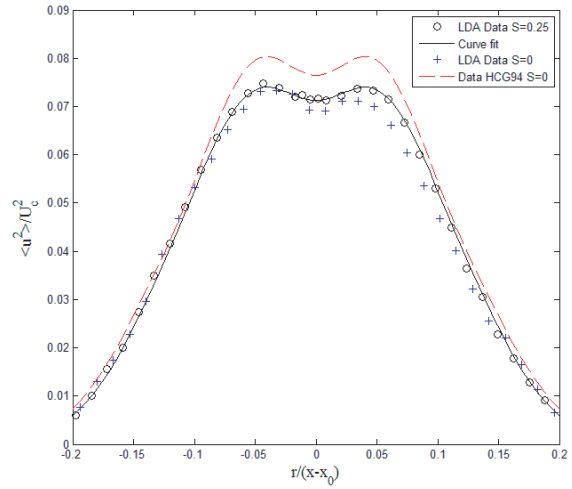

(a) Normalized $\overline{u^2}$

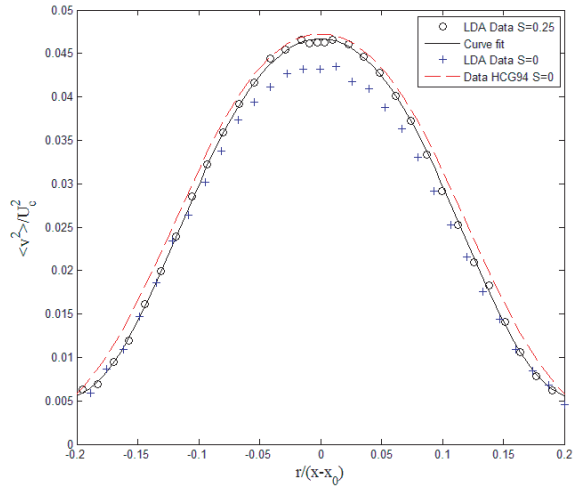

(b) Normalized $\overline{v^2}$

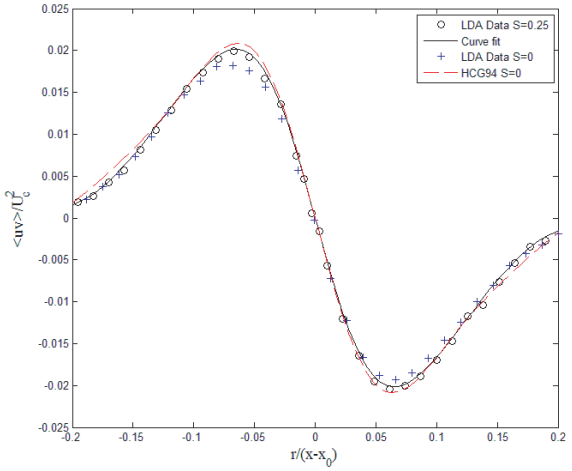

(c) Normalized $\overline{uv}$

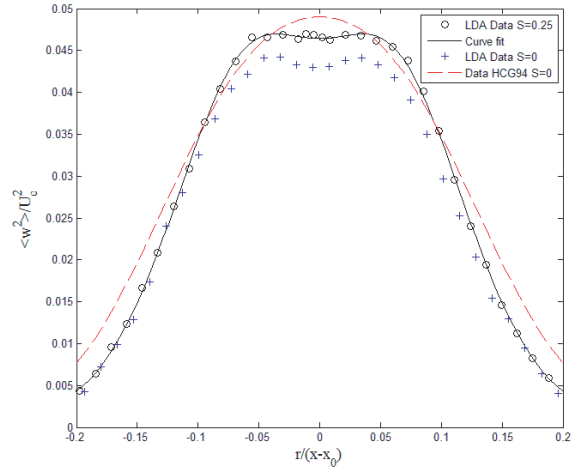

(d) Normalized $\overline{w^2}$

Figure 3: Second-Order Moments at $x/D = 30$, compared with non-swirling jet data from HCG [5].

Energy Balance and Dissipation

If the pressure-velocity correlations and dissipation were known it would be possible to calculate the other terms by using turbulence kinetic energy equation as below:

$$U\frac{\partial k}{\partial x} + V\frac{\partial k}{\partial r} = -\left[\frac{\partial}{\partial x}\left(\frac{1}{\rho}\overline{pu} + \frac{1}{2}\overline{q^2 u} - \nu\frac{\partial k}{\partial x}\right) + \frac{1}{r}\frac{\partial}{\partial r}r\left(\frac{1}{\rho}\overline{pv} + \frac{1}{2}\overline{q^2 v} - \nu\frac{\partial k}{\partial r}\right)\right] - \left[\overline{uv}\left(\frac{\partial U}{\partial r} + \frac{\partial V}{\partial x}\right) + \overline{u^2}\frac{\partial U}{\partial x} + \overline{v^2}\frac{\partial V}{\partial r} + \overline{w^2}\frac{V}{r}\right] - \epsilon \tag{7}$$

In the present experiment we were not able to directly measure the dissipation, therefore, the velocity-pressure correlation terms $\frac{1}{\rho}\overline{pv}$ and $\frac{1}{\rho}\overline{pu}$ in the equation 7 could not be inferred directly as in Hussein et al. [5]. The streamwise gradient of $\overline{pu}/\rho$ can be ignored relative to the radial gradient of $\overline{pv}/\rho$. Also, Hussein et al. [5] showed from a locally axisymmetric dissipation, radial gradient has the same shape as $\overline{q^2 v}$, consistent with the estimate of Lumley [10] that $-\overline{pv}/\rho = (\frac{1}{5})\overline{q^2 v}$. Also the coincident moment of tangential and radial velocity components, $\overline{uw}$, was not measured because of the two-component LDA measurement. In the energy balance computation it was assumed that $\overline{vw^2} \equiv \overline{v^3}$. We are able to calculate the dissipation through kinetic energy equation. The normalized kinetic energy balance is plotted in figure 5. The results are virtually indistinguishable from those of Hussein et al. [5].

The component Reynolds stress equations for the jet are given as below [9]:

- $\overline{u^2}$ *Balance:*

$$U\frac{\partial \overline{u^2}}{\partial x} + V\frac{\partial \overline{u^2}}{\partial r} = \left[2\overline{\frac{p}{\rho}\frac{\partial u}{\partial x}}\right] - \left[2\overline{uv}\frac{\partial U}{\partial r} + 2\overline{u^2}\frac{\partial U}{\partial x}\right] - \left[\frac{\partial \overline{u^3}}{\partial x} + \frac{\overline{u^2 v}}{r} + \frac{\partial \overline{u^2 v}}{\partial r}\right] - 2\epsilon_{xx} \tag{8}$$

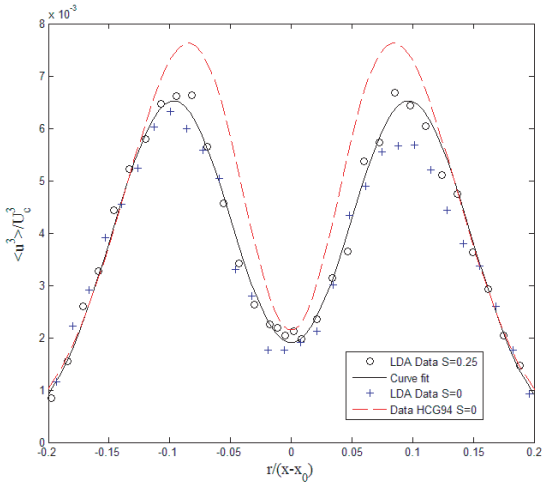

(a) Normalized $\overline{u^3}$

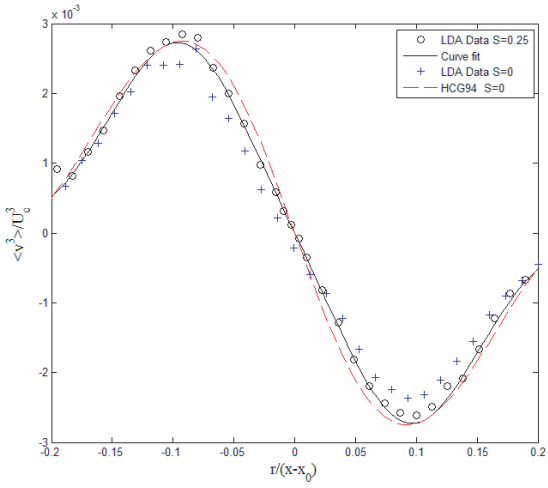

(b) Normalized $\overline{v^3}$

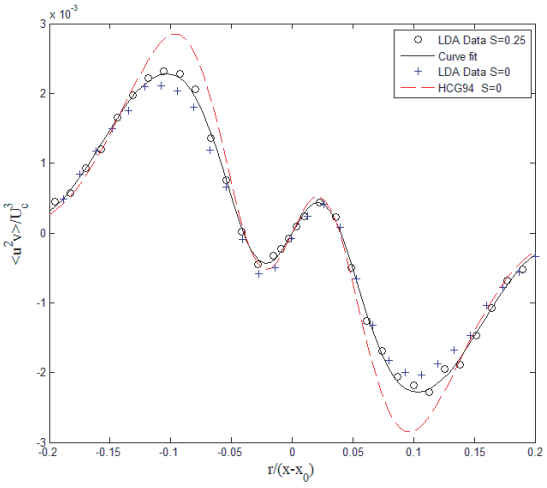

(c) Normalized $\overline{u^2 v}$

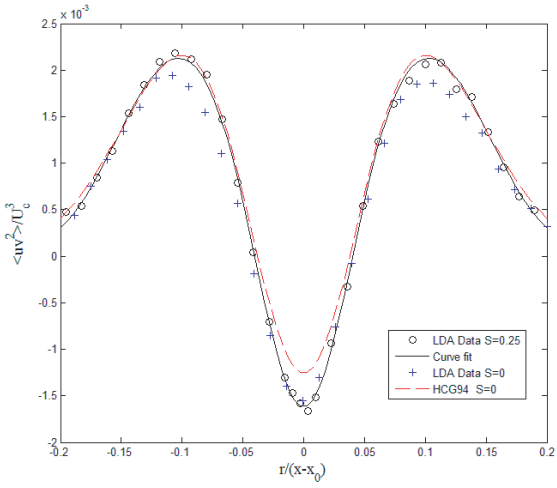

(d) Normalized $\overline{uv^2}$

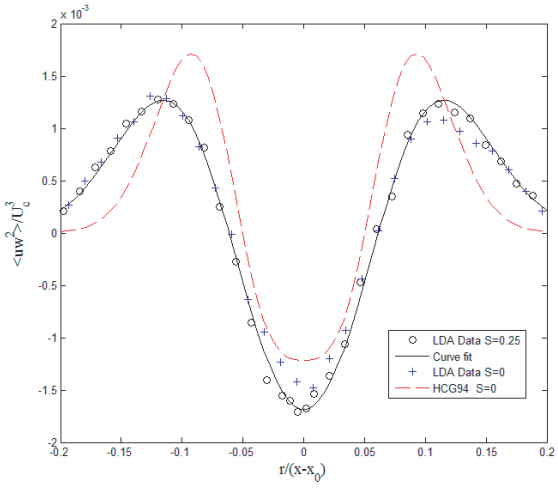

(e) Normalized $\overline{uw^2}$

Figure 4: Third-Order Moments at $x/D = 30$, compared with non-swirling jet data from HCG [5].

- $\overline{v^2}$ *Balance:*

$$U\frac{\partial \overline{v^2}}{\partial x} + V\frac{\partial \overline{v^2}}{\partial r} = \left[2\frac{\overline{p}}{\rho}\frac{\partial \overline{v}}{\partial r} - \frac{2}{\rho}\frac{\partial \overline{pv}}{\partial r}\right] - \left[2\overline{v^2}\frac{\partial V}{\partial r} + 2\overline{uv}\frac{\partial V}{\partial x}\right] - \left[\frac{\overline{v^3}}{r} + \frac{\partial \overline{v^3}}{\partial r} - 2\frac{\overline{vw^2}}{r} - 4W\frac{\overline{vw}}{r} + \frac{\partial \overline{uv^2}}{\partial x}\right] - 2\epsilon_{rr} \tag{9}$$

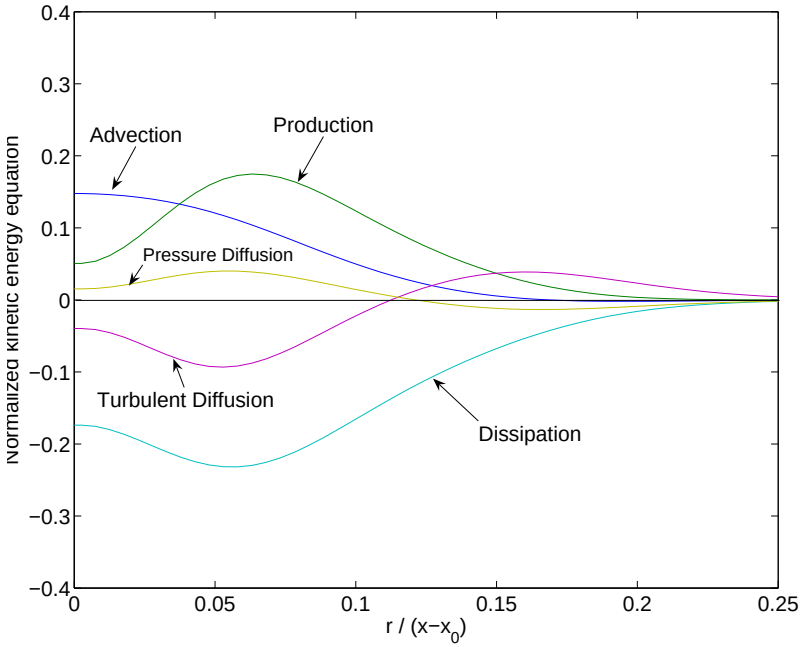

Figure 5: Kinetic energy balance normalized by $U_c^3/(x-x_0)$.

- $\overline{w^2}$ *Balance:*

$$U\frac{\partial\overline{w^2}}{\partial x}+V\frac{\partial\overline{w^2}}{\partial r}=\left[\frac{2}{r}\overline{\frac{p}{\rho}\frac{\partial w}{\partial\theta}}\right]-\left[2\overline{uw}\frac{\partial W}{\partial x}+2\overline{vw}\frac{\partial W}{\partial r}\right]-\left[\frac{\partial\overline{uw2}}{\partial x}+\frac{\partial\overline{vw^2}}{\partial r}+3\frac{\overline{vw^2}}{r}+2\overline{vw}\frac{W}{r}+2\overline{w^2}\frac{V}{r}\right]-2\epsilon_{\theta\theta} \tag{10}$$

- $\overline{uv}$ *Balance:*

$$\begin{aligned}U\frac{\partial\overline{uv}}{\partial x}+V\frac{\partial\overline{uv}}{\partial r}=&\left[\overline{\frac{p}{\rho}\left(\frac{\partial v}{\partial x}+\frac{\partial u}{\partial r}\right)}\right]-\left[\overline{uv}\left(\frac{\partial U}{\partial x}+\frac{\partial V}{\partial r}\right)+\overline{v^2}\frac{\partial U}{\partial r}+\overline{u^2}\frac{\partial V}{\partial x}\right]\\&-\left[\frac{\partial\overline{u^2v}}{\partial x}+\frac{\partial\overline{uv^2}}{\partial r}+\frac{\overline{uv^2}}{r}-\frac{\overline{uw^2}}{r}-2\overline{uw}\frac{W}{r}\right]-2\epsilon_{xr}\end{aligned} \tag{11}$$

The locally axisymmetric estimate is suggested by Hussein et al. [5] to best represent the dissipation in the jet flow. But because we could not measure the dissipation directly for each Reynolds stress equation, the only possible hypothesis is to assume isotropic dissipation distribution; i.e., $\epsilon_{xx}=\epsilon_{rr}=\epsilon_{\theta\theta}=\epsilon/3$ and $\epsilon_{xr}=\epsilon_{r\theta}=\epsilon_{x\theta}=0$. The energy balances for Reynolds stresses are plotted in figure 6. The values are normalized by cube of the centerline velocity over distance from nozzle. x_0 is the virtual origin of the swirling jet as shown in figure 1. The graphs are in a good agreement with the earlier non-swirling jet energy balance of Hussein et al. [5].

CONCLUSIONS

An investigation on turbulent transport equations in the self-preserving region of a moderate swirling jet flow has shown that the role of different terms in energy balance has not been affected by the additional azimuthal velocity component at the exit of jet. As previously noted by Shiri et al. [2], the mean stream-wise velocity for swirling jet has the same rate of evolution as non-swirling jet with the same initial condition. The higher-order moments in the swirling jet flow also shows this similarity. The slight differences observed in some moments like $\overline{u^2}$ could be the effect of exit profile which tends to change when azimuthal component is added to the jet, or could be simply due to differences in the measurement methodology. The quantities measured and calculated in this study are essential for evaluating turbulence closure models, an effort which is already in progress.

ACKNOWLEDGEMENTS

The authors are especially grateful to Dr. J. Naughton for his helpful advice and counsel. Dr. D. Ewing also provided useful insight and comments.

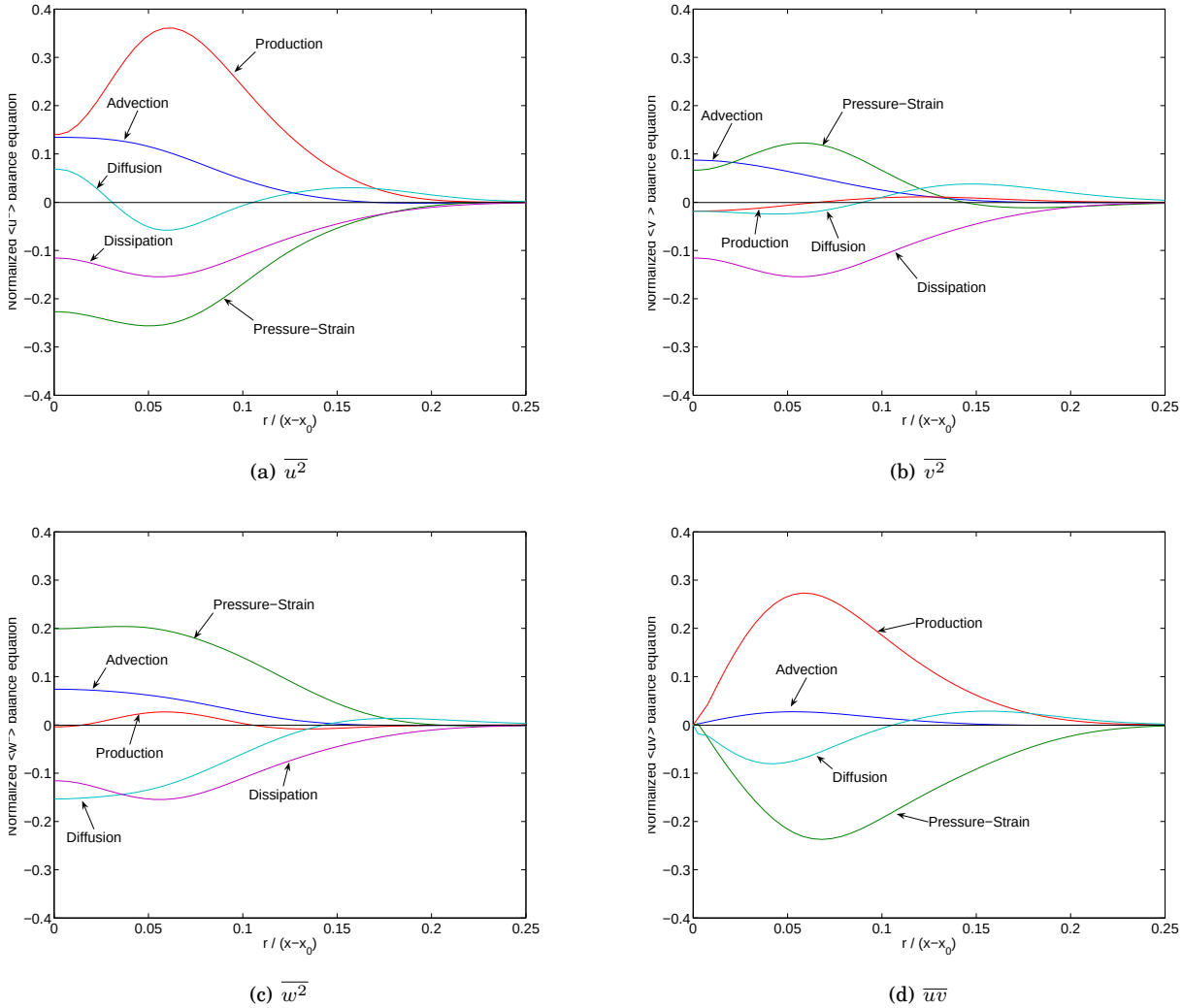

(a) $\overline{u^2}$ (b) $\overline{v^2}$

(c) $\overline{w^2}$ (d) $\overline{uv}$

Figure 6: Reynolds stress balance equations normalized by $U_c^3/(x - x_0)$.

References

[1] A. Shiri, S. Toutiaei and W.K. George, *Turbulent Flow Structure in the Similarity Region of a Swirling Jet.* Proceedings of the 11th European Turbulence Conference, June 2007 Portugal.

[2] A. Shiri, W.K. George and J.W. Naughton, *An Experimental Study of the Far-Field of Incompressible Swirling Jets.* 36th AIAA Fluid Dynamics Conference and Exhibit, AIAA 2006-3367

[3] R.T. Gilchrist and J.W. Naughton, *Experimental Study of Incompressible Jets with Different Inital Swril Distributions: Mean Results.* AIAA Journal, Vol 43, p: 741-751, April 2005

[4] D. Ewing *Decay of Round Turbulent Jets with Swirl.*, Proceedings of the 4th International Symposium on Engineering Turbulence Modeling and Experiments, Elsvier, 1999

[5] H.J. Hussein, S.P. Capp and W.K. George, *Velocity Measurements in a High-Reynolds-number, Momentum-Conserving, Axisymmetric, Turbulent Jet.* Journal of Fluid Mechanics, Vol 258, p: 31-75, 1994

[6] N.R. Panchapekesan and J.L. Lumley, *Turbulence Measurements in Axisymmetric Jets of Air and Helium. Part1. Air Jet.* Journal of Fluid Mechanics, Vol 246, p: 197-223, 1993

[7] S. Farokhi, R. Taghavi and E.J. Rice, *Effect of Initial Swirl Distribution on the Evolution of a Turbulent Jet.* AIAA Journal, Vol 27, No. 6, p: 700-706, 1989

[8] W.K. George, *The self-preservation of turbulent flows and its relation to initial conditions and coherent structures.* Advances in Turbulence, p: 39-73, Hemisphere, NY, 1989

[9] M.M. Gibson and B.A. Younis, *Calculation of Swirling Jets with a Reynolds Stress Clouser*. Physics of Fluids, Vol 29, p: 38-48, 1986

[10] J.L. Lumley, *Computational Modeling of Turbulent Flow*. Advances in Applied Mechanics, Vol 18, p: 123-176, 1978